A Vertical Methodology for the Design Space Exploration of Graphene-enabled Wireless Communications

Sergi Abadal*
NaNoNetworking Center in Catalonia
UPC - BarcelonaTech
Barcelona, Spain

Albert Mestres
NaNoNetworking Center in Catalonia
UPC - BarcelonaTech
Barcelona, Spain

Ignacio Llatser
Vodafone Chair for Mobile Communication Systems
TU Dresden
01062 Dresden, Germany

Eduard Alarcón
NaNoNetworking Center in Catalonia
UPC - BarcelonaTech
Barcelona, Spain

Albert Cabellos-Aparicio
NaNoNetworking Center in Catalonia
UPC - BarcelonaTech
Barcelona, Spain

ABSTRACT

Graphene-based antennas (or shortly named, *graphennas*) are envisaged to be the cornerstone of novel wireless communication systems by virtue of their reduced size, in the micrometer range, and an expected radiation frequency of a few terahertz. Progress in the characterization of graphennas and terahertz propagation indicate that nanoscale phenomena will significantly impact on the performance of such graphene-enabled wireless communication systems. Motivated by this fact and the novelty of the investigations, a methodology for the early-stage exploration of the performance of graphene-enabled wireless links is proposed in this paper. The novelty of this methodology resides in its highly vertical approach, which aims to bridge the wide conceptual gap between nanoscale physics and time-domain physical layer modeling and design. With it, the performance of a graphene-enabled wireless link is evaluated as a function of the chemical potential of graphene, the composition of the propagation medium, and the transmission distance in a simple case scenario.

Categories and Subject Descriptors

C.2.1 [**Computer-Communication Networks**]: Network Architecture and Design—*Wireless Communication*; C.2.m [**Computer-Communication Networks**]: Miscellaneous

Keywords

Graphene-based Antennas, Terahertz, Physical Layer Modeling, Time-Domain Analysis, Impulse Radio, Molecular Absorption, Carrier Mobility, Chemical Potential

*Corresponding email: abadal@ac.upc.edu

NANOCOM '15, September 21 - 22, 2015, Boston, MA, USA

DOI: http://dx.doi.org/10.1145/2800795.2800815

1. INTRODUCTION

Nanotechnology is enabling the development and manufacture of systems with nanometric precision, leading not only to a further miniaturization of existing systems, but also to the creation of new systems that take advantage of the unique characteristics of nanomaterials [4]. Within this context, novel applications may require smaller forms of wireless communication while maintaining certain application-dependent performance in terms of bandwidth, transmission range or energy consumption: Wireless Networks-on-Chip (WNoCs) [1, 6] and Wireless NanoSensor Networks (WNSNs) [3] are two clear examples. On the one hand, the WNoC paradigm consists in placing multiple antennas within the same chip to wirelessly communicate its internal components, thereby addressing several performance challenges of current interconnects. On the other hand, WNSNs aim to enable wireless communication among nanosensors, seeking to exploit their novel sensing capabilities in locations not reachable with conventional sensors or in scenarios requiring a very high accuracy or deployment density.

In both cases, evident area constraints impose the use of antennas a few micrometers in size: nanosensors are a few micrometers in size as well, whereas chip area is a primary design constraint in WNoCs and must be minimized. To meet such stringent size requirements, graphene-based plasmonic antennas [11, 14] and transceivers would be a valid alternative to downscaled versions of conventional RF units due to their unique properties. A graphene-based antenna several micrometers long is able to radiate in the terahertz band (0.1 - 10 THz) with reasonable efficiency, whereas its same-size metallic counterpart would resonate in the near infrared and optical bands instead, which are not suitable for RF wireless communications due to attenuation and transceiver complexity issues.

Scaling down the size of the communication units (and the wavelengths) intuitively implies that nanoscale principles will largely determine the communication performance. As a result, it is important to carefully consider the impact of nanoscale phenomena upon performance even if communication occurs at much larger scales. In light of the disjoint nature of both extremes, there is a need for vertical methodologies that explicitly bridge the conceptual gap

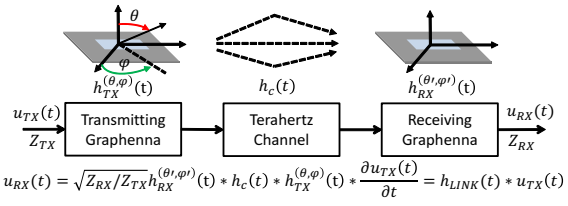

Figure 1: Time-domain physical layer model.

between the disciplines involved. By expressing communication performance as a function of variables that define nanoscale physics through models, design space explorations can be performed during early development stages. As models evolve and improve, such methodologies would allow to obtain accurate evaluations of communication performance before graphene antennas are implemented and experimental testbeds are available.

In this paper, we propose a vertical methodology for the evaluation of graphene-enabled wireless communications in the terahertz band as a function of the nanoscale phenomena uniquely relevant to the scenario. Motivated by the high radiation frequency, the potentially wideband nature of such communications, and the envisaged use of impulse-based modulations [12], the proposed methodology employs time-domain characterization techniques [16, 19]. It represents a direct extension of our previous works, where the impact of the physics of graphene upon the performance of graphene-based antennas [2] and the effects of molecular absorption upon the propagation of terahertz signals [15] were analyzed in the time domain and from a communications perspective. This framework incorporates the methods used there, as well as in other comprehensive research efforts [7], towards a parametrized end-to-end physical model for graphene-enabled wireless communications in the terahertz band. The main novelty of the work does not reside in the proposed performance metrics, but in the vertical bridge that is built between physical layer metrics and the nanoscale phenomena inherent to this novel scenario.

The remainder of this paper is as follows. In Sec. 2, we explain the proposed methodology. In Sec. 3, we particularize it for a simple case study, seeking to evaluate the impact of the chemical potential of graphene and the molecular absorption of the medium upon the performance of a graphene-enabled wireless link. Sec. 4 concludes the paper.

2. A METHODOLOGY FOR THE ANALYSIS OF A GRAPHENE-ENABLED WIRELESS LINK IN THE TIME DOMAIN

Fig. 1 shows the model of a wireless link, which relates the voltage $u_{RX}(t)$ at the output terminals of the receiving antenna with the input voltage $u_{TX}(t)$ delivered at the terminals of the transmitting antenna. We follow the formulation and considerations used in [19] for the time-domain characterization of ultra-wideband (UWB) systems.

Assume that characteristic impedance of the feeds at the transmitting and receiving antennas are Z_{TX} and Z_{RX}, respectively. Then, the output voltage is:

$$\frac{u_{RX}(t)}{\sqrt{Z_{RX}}} = h_{RX}^{(\theta',\phi')}(t) * h_c(t) * h_{TX}^{(\theta,\phi)}(t) * \frac{\partial}{\partial t}\frac{u_{TX}(t)}{\sqrt{Z_{TX}}}, \quad (1)$$

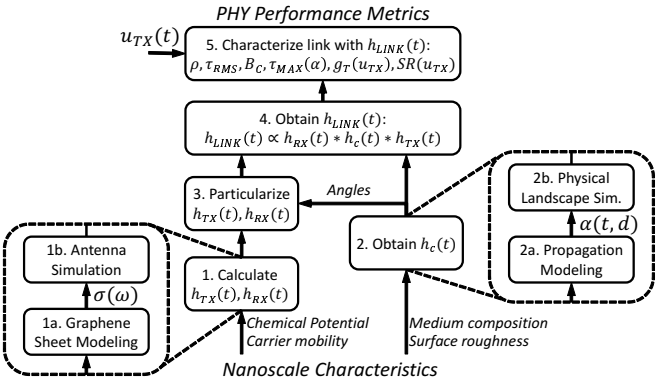

Figure 2: Vertical methodology for the time-domain characterization of graphene-enabled wireless links as functions of nanoscale phenomena.

where $h_{TX}^{(\theta,\phi)}(t)$ and $h_{RX}^{(\theta',\phi')}(t)$ are the impulse responses of the transmitting and receiving antennas for a given polarization and at the direction determined by the pair of angles $\{\theta, \phi\}$ and $\{\theta', \phi'\}$, respectively, and for a given polarization. $h_c(t)$ is the transient response of the propagation channel, whereas the operands $*$ and $\frac{\partial}{\partial t}$ represent convolution and time derivative. The impulse response of the whole link $h_{LINK}(t)$ (channel and antennas) can be calculated by assuming that $u_{TX}(t) = \delta(t)$ and applying the properties of the convolution operation:

$$h_{LINK}(t) = \sqrt{\frac{Z_{RX}}{Z_{TX}}}\frac{\partial}{\partial t}(h_{RX}^{(\theta',\phi')}(t) * h_c(t) * h_{TX}^{(\theta,\phi)}(t)). \quad (2)$$

A similar reasoning can be followed in the frequency domain. With the transfer function of the different elements, we can calculate the frequency response of the link as:

$$H_{LINK}(f) = j\omega\sqrt{\frac{Z_{RX}}{Z_{TX}}}H_{RX}^{(\theta',\phi')}(f)H_c(f)H_{TX}^{(\theta,\phi)}(f), \quad (3)$$

to then obtain $h_{LINK}(t)$ by applying the inverse Fourier transform.

The main objective of the proposed methodology is to provide means to characterize the graphene-enabled wireless link in the time domain through its impulse response $h_{LINK}(t)$. As summarized in Fig. 2, five steps are required to this end:

1. To obtain the transient response of the transmitting and receiving antennas $h_{TX}^{(\theta,\phi)}(t)$ and $h_{RX}^{(\theta',\phi')}(t)$ as a function of the characteristics of the underlying graphene sheets, using the methods outlined in Sec. 2.1.
2. To calculate the impulse response of the channel $h_c(t)$ as a function of the propagation medium and of the physical landscape, as indicated in Sec. 2.2.
3. To particularize the response of the antennas for the angles of radiation and arrival obtained in step 2.
4. To use the impulse response of the antennas and the channel to evaluate $h_{LINK}(t)$ via Eqs. (2) or (3).
5. To characterize the communication performance of the link through a set of time-domain metrics summarized in Sec. 2.3.

It is important to emphasize that, following these steps, we are able to express the different performance metrics as a function of the target parameters representing nanoscale characteristics of the antennas or the channel. This is the main aim and contribution of the proposed methodology.

2.1 Impulse Response of the Antenna

Signals fed to any antenna are generally subject to differentiation, dispersion, radiation, and losses. At the receiving end, signals suffer from additional dispersion and losses. As pointed out above, these effects are modeled with either a transient response $h(t)$ or a transfer function $H(f)$, both dependent on the direction of radiation or incidence. From Eq. (1), it is observed that the model used in this work leaves the time derivative out of the impulse response of the antenna, as opposed to in [17], thus decoupling the differentiation effects inherent to all antennas from other antenna-dependent phenomena. Following this definition, the reciprocity theorem yields $h_{TX}(t) = h_{RX}(t)$ and $H_{TX}(f) = H_{RX}(f)$ for the same antenna [19]. Note that this also applies in the case of graphene-based antennas, since the same plasmonic principles explain their operation in both ends [11].

Graphene-based antennas, in essence, consist of a number of finite-size graphene layers (the radiating elements) mounted over a metallic flat surface (the ground plane), with a dielectric material in-between and a feed to drive the signals to the antenna. As outlined in Fig. 2, obtaining the impulse response of such a structure implies modeling the graphene sheets and then simulating the entire antenna structure. Here, we summarize the main specifities of this process; we refer the reader to [2] for more details.

Modeling the graphene structure: the frequency characteristics of the electric conductivity of graphene is the main determinant of the properties of the plasmonic phenomena that occur within graphene-based antennas. The complexity of the models used to calculate it will depend on the frequency band of interest and the characteristics of the graphene sheet, since they determine which effects (e.g. damping) should be taken into consideration [5]. Considering a graphene patch a few micrometers in size and an expected radiation frequency in the terahertz band, the Kubo formalism can be used:

$$\sigma(\omega) = \frac{2e^2}{\pi\hbar}\frac{k_B T}{\hbar}\ln\left[2\cosh\left[\frac{E_F}{2k_B T}\right]\right]\frac{i}{\omega + i\tau^{-1}}, \quad (4)$$

where e, $\hbar$, and k_B are the charge of an electron, the reduced Planck constant, and the Boltzmann constant, respectively [8]. Variables T, $\tau \approx f(\mu)$, and E_F correspond to the temperature, the relaxation time (a function of the carrier mobility μ), and the chemical potential of the graphene layer. As thoroughly explained in [2], these variables can be considered as design parameters and will be of interest when studying the performance at the physical layer.

Simulating the antenna: once the frequency-dependent conductivity of graphene is calculated, the radiating element of the antenna can be rigorously modeled as an infinitesimally thin surface with an equivalent impedance of $Z(\omega) = \frac{1}{\sigma(\omega)}$. The graphene layer needs to be shaped according to antenna geometry and then integrated within the target antenna configuration; the complexity and accuracy of the models used to describe it are design decisions and will depend on the focus of the study. By means of an electromagnetic simulator, we can either calculate the fields radiated by the antenna as a function of the input voltage in transmission, or consider a wave incident to the antenna and calculate the voltage at the antenna terminals in reception. The response of the antenna is obtained by relating the voltage and the electromagnetic fields, as detailed in [2, 19]. Simulators commonly offer methods to perform this in both domains; in case the response is obtained in the frequency domain, it is necessary to apply the inverse Fourier transform as $h(t) = \mathcal{F}^{-1}(H(\omega))$.

2.2 Impulse Response of the Channel

The impulse response of the channel $h_c(t)$ accounts for the different phenomena that attenuate and disperse the signal during propagation. These can be inherent to the propagation medium, or result from the interaction of signals with the elements located between transmitter and receiver. In general, they can be mathematically represented as:

$$h_c(t) = \sum_{i=1}^{L} \alpha_i^{-1}(t,d) e^{j\varphi_i(t,d)} \delta(t - \tau_i), \quad (5)$$

where d denotes separation between transmitter and receiver and L is the number of components that reach the receiving antenna. This equation basically expresses that signals will suffer, for each path to the receiver, a given attenuation α, a phase shift φ and a delay τ.

As summarized in Fig. 2 and according to Eq. (5), calculating the impulse response of the channel implies modeling the propagation medium to assess the attenuation and phase shift per unit of distance, and then simulating the physical landscape in order to obtain the number, distribution, and characteristics of multipath components.

Modeling the propagation medium: When considering free space propagation through air, we normally have that $\alpha(t,d) = (2\pi d c_0)^{-1}$, $\phi(t,d) = 0$ and $\tau(t,d) = d/c_0$ with c_0 representing the speed of light [19]. However, terahertz waves are susceptible to molecular effects negligible in lower frequencies [10, 13, 15]. Basically, electromagnetic waves *A)* excite gas molecules whose resonant frequency is in the terahertz band, losing energy in the process (molecular absorption), and *B)* are scattered by particles whose size is comparable to the wavelength of the signal (small-particle scattering). These effects are frequency-selective and, therefore, have an impact upon the response of the channel in both domains. Specifically, we have:

$$\alpha(f,d) = \frac{e^{k(f)d}}{2\pi d c_0}, \quad \alpha(t,d) = \mathcal{F}^{-1}(\alpha(f,d)), \quad (6)$$

where $k(f) = \sum_j k_a^j + k_s^j$ is the extinction loss coefficient, which accounts for the molecular absorption and scattering contributions of all the elements present in the medium through the coefficients k_a and k_s, respectively. These coefficients model the quantity of molecular absorption and scattering per type of molecule. Therefore, the particular mixture of molecules that waves will find along its path, as well as the transmission distance, will be the two main determinants of the propagation loss. We refer the reader to [13] for more details and refined models.

Simulating the physical landscape: the scenarios must be modeled and simulated using techniques such as ray tracing (full-EM simulations become too costly) to obtain the

multipath behavior of the channel. The outcome of these simulations will depend on the application scenario: most applications generally require of an statistical model comprehending the most representative settings in terms of obstacle shape, composition, or motion [16]. In other applications, e.g. intra-chip wireless networks, the scenario is static and can be not only known *a priori*, but even modified at design time to optimize certain metrics. For instance, the characteristics of the dielectric used throughout the chip can be tuned as they have an impact upon performance [18].

As thoroughly analyzed in [7], the channel characterization for wireless communications in the terahertz band has a particularity besides the presence of molecular effects inherent to the propagation. In case surfaces present a roughness comparable to the wavelength of the signal, diffuse scattering appears when the signal is reflected. Given the small wavelength of terahertz waves, such diffuse scattering effects cannot be neglected anymore and need to be considered [9].

2.3 Performance Metrics

The final step in our methodology is to employ the impulse response $h_{LINK}(t)$ to fully characterize the link at the physical layer. Since $h_{LINK}(t)$ contains antenna and channel effects, the metrics generally used to separately characterize both aspects would be valid. Our previous work [2] particularizes a family of time-domain antenna characterization metrics for the graphene-enabled wireless communication scenario; whereas terahertz band research by Han, Ozan Bicen and Akyildiz uses UWB channel characterization methods based on the power delay profile [7]. The novelty resides in how the methodology is capable to expressing these metrics as functions of nanoscale phenomena.

It is important to note that, while using different formulation, both research lines refer to the same phenomena and effects: attenuation and dispersion are analyzed by evaluating, respectively, the characteristics in terms of amplitude and temporal length of the response. Since the channel is included in the analysis, we propose to use the power delay profile (PDP, $p(t)$). It is calculated as:

$$p(t) = |h_{LINK}(t)|^2. \tag{7}$$

To characterize the PDP, we will use typical metrics such as the maximum excess delay and the RMS delay spread. Additionally, we propose two antenna-oriented metrics in order to characterize the response of the whole link in the presence of a given input waveform: the transient gain and the pulse width stretch ratio.

Response Peak the peak ρ of the response is the maximum value of the PDP:

$$\rho = \max_t p(t), \tag{8}$$

with $1/\rho$ representing a lower bound of the attenuation introduced by the link. A high value of ρ is desired, as receiving a strong peak allows for a precise detection of the pulse position, which is desirable in location, ranging, and coherent communication applications.

RMS Delay Spread / Coherence Bandwidth: the RMS delay spread is the square root of the second central moment of the PDP, given as:

$$\tau_{RMS} = \sqrt{\int (t - \tau_m)^2 \cdot p(t)}, \tag{9}$$

where $\tau_m = \int t \cdot p(t)$ is the mean excess delay. Also, the RMS delay spread is inversely proportional to the coherence bandwidth B_C of the link. The RMS delay spread is a measure of the time dispersion introduced by the frequency selectivity of, in our methodology, both the channel and the antenna. Similarly, the coherence bandwidth measures the frequency interval over which the response does not change significantly, giving a hint of the available bandwidth. Low values of the delay spread are desired, as this implies that the link admits the transmission of short pulses towards obtaining high data rates.

Maximum Excess Delay: this metric is generally defined with respect to a parameter α that represents the signal level below which the received signal can be neglected:

$$\tau_{max}(\alpha) = \{t' \,:\, t' > t_\rho \wedge p(t') = \alpha \cdot \rho\} \tag{10}$$

where rho is the response peak given by Eq. (8) and t_ρ is delay at the response peak. It gives further information on the spreading characteristics of both the channel (due to multipath) and the antenna (due to ringing).

Transient Gain: the transient gain g_T, in its conventional form, is the time domain version of the antenna gain. Here, we propose to extend it in order to cover the whole link, defining it as the ratio of power at the receiver to power at the transmitter. Given that the power of a given waveform $u_X(t)$ is $P_X = \|u_X(t)\|^2/Z_X$, the transient gain is:

$$g_T(u_{TX}) = \frac{P_{RX}}{P_{TX}} = \frac{Z_{TX}}{Z_{RX}} \frac{\|h_{LINK}(t) * u_{TX}(t)\|^2}{\|u_{TX}(t)\|^2}, \tag{11}$$

where the norm is $\|f(x)\| = \int_{-\infty}^{\infty} |f(x)|dx$. The transient gain is an indicator of how efficiently a given link is able to transmit a given signal u_{TX}. It is specially relevant since a design objective is to maximize the power that reaches the receiver towards reducing the error rate.

Pulse Width Stretch Ratio: similarly to the transient gain, the stretch ratio SR is defined with respect an input waveform. Let the normalized cumulative energy function of a given signal $s(t)$ be defined as $E_s(t) = \int_{-\infty}^{t} |s(t)|^2/\|s(t)\|^2$. Assuming that a certain fraction α of energy can be neglected, the width of the signal $W(s)$ can be then obtained with the following equation:

$$W(s) = E_s^{-1}(1 - \alpha/2) - E_s^{-1}(\alpha/2). \tag{12}$$

The stretch ratio is obtained by dividing the width of the radiated pulse by the width of the input waveform:

$$SR(u_{TX}) = \frac{W(h * \frac{\partial u_{TX}}{\partial t})}{W(u_{TX})}. \tag{13}$$

Therefore, the pulse width stretch ratio quantifies the broadening of a pulse caused by the antennas and the channel. A value close to 1 is desired, since an important design target is to minimize the broadening of pulses leading to higher transmission rates.

3. CASE STUDY

To exemplify the use of the proposed methodology, here we particularize it for a simple case study. We choose a simple scenario as the focus of this paper is the definition of the vertical framework. In future work, we plan to use the methodology to explore more compelling case scenarios.

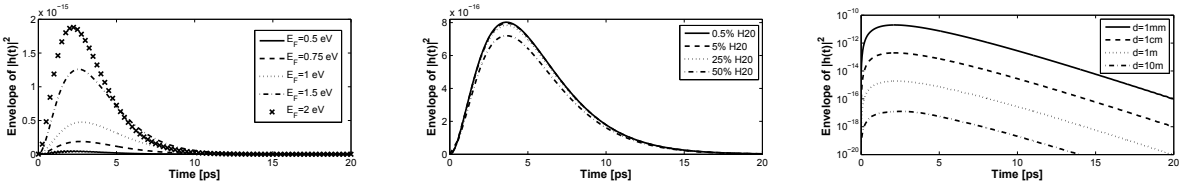

(a) μ=4m^{2}V^{-1}s^{-1},10% H_2O, d=1m (b) E_F=1eV, μ=12m^{2}V^{-1}s^{-1}, d=1m (c) E_F=2eV, μ=4m^{2}V^{-1}s^{-1}, 10% H_2O

Figure 3: Envelope of the PDP for different antenna, medium and landscape possibilities.

The link to be explored has the following characteristics and parameters:

- *Antennas:* we assume a 5-µm by 1-µm graphene-based antenna, with a fixed carrier mobility of $\mu = 4m^2V^{-1}s^{-1}$) and variable chemical potential. In transmission, the antenna is fed with a 1-THz wide sinc pulse centered at the resonant frequency of the antenna.
- *Medium:* the medium is air with variable vapor concentration. Small-particle scattering is negligible.
- *Landscape:* we assume that antennas are face to face and, therefore, line-of-sight propagation will take place through the boresight direction of the antennas. Transmission distance is variable.

Figure 3 shows the PDP of the link under investigation for different (a) graphene chemical potentials, (b) water vapor percentage, and (c) distances. Firstly, it is observed that increasing the chemical potential clearly impacts upon the response as both the amplitude and relative width of the response grow as well. This is due to the improvement in terms of the resonant behavior of the graphenna [2]. The second plot infers that, for the graphenna with E_F=1eV and μ=12m^{2}V^{-1}s^{-1}, the presence of water vapor has a scarce impact on the response unless the levels of water vapor reach unrealistic limits above 5%. This is because the family of graphennas considered here resonate at frequencies lower than those where molecular absorption is significant, at least for distances below 10 meters [15]. Finally, the third plot (note the log scale in the Y-axis) shows the dependence of the response with the distance. These results include both the typical dependence with the square of the distance due to spreading losses, as well as a small yet non-negligible molecular absorption that also increases with distance.

3.1 Attenuation Analysis

Given that reasonable amounts of water vapor have a reduced impact upon the attenuation of the links assessed here, we will only evaluate losses with respect to the choice of antenna and scenario. Figure 4 shows the response peak and the transient gain as functions of the chemical potential and transmission distance. Both follow almost identical tendencies, probably due to the fact that the bandwidth of the input pulse is higher than that of the antenna in all cases. It is observed that the chemical potential increase is very beneficial up to around 1 eV; above this level the gain stabilizes. Also, note that the dependency with respect to the distance may also vary with chemical potential. In both cases, this is because a change in the latter implies a variation in the resonant frequency of the antenna.

3.2 Dispersion Analysis

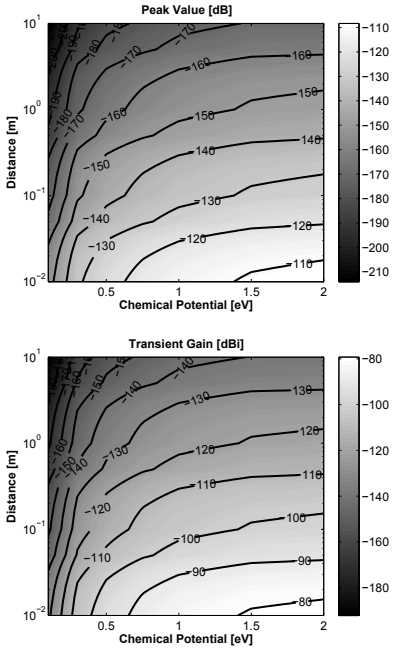

Figure 4: Response peak (top) and transient gain (bottom) for different chemical potentials and transmission distances, with μ=4m^{2}V^{-1}s^{-1} and 10% H_2O.

In light that the dispersion does not heavily depend either on the medium composition or the transmission distance, at least for the conditions assumed in this work, we evaluate it as a function of the chemical potential. Figure 5 shows the excess delay and pulse width stretch ratio as functions of the chemical potential. Both follow tendencies very similar to that of the attenuation with respect to the chemical potential, increasing up to around 1eV and then stabilizing or even decreasing. This is given by the behavior of the antenna in the different cases: as the chemical potential increases, the antenna presents a more pronounced resonance, which increases the efficiency but slightly reduces the relative bandwidth. Such bandwidth reduction will cause a temporal broadening of the input pulse, which results in the stretch ratio figures obtained here.

4. CONCLUSIONS

We presented a vertical methodology for the early-stage exploration of graphene-enabled wireless links. It basically consists in calculating the impulse response of the antenna and channel combination as a function of nanoscale physical parameters, which allows designers to relate these pa-

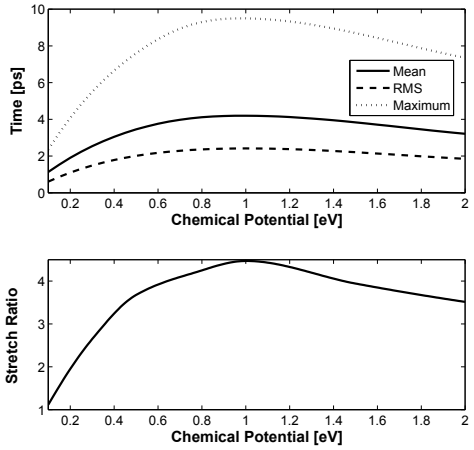

Figure 5: Excess delay statistics (top) and pulse width stretch ratio (bottom) for different chemical potentials, with μ=4m^{2}V^{-1}s^{-1}, 10% H_2O, and d=1m.

rameters to a set of performance metrics. Following this methodology, we observed that an increase in the chemical potential of a resonant graphenna leads to an improvement in terms of attenuation, but has a negative impact in terms of dispersion. Even though we also showed that spreading losses dominate for the link under investigation, molecular absorption must not be neglected given its frequency-selective nature and the relation between chemical potential of a graphenna and its resonant frequency. In future work, we plan to take these initial considerations into account to analyze more complex case scenarios, e.g. graphene-enabled wireless communication in on-chip environments. Further investigations could extend the proposed methodology to, for instance, assist the design of pulse generators through the optimization of the input-dependent metrics, or to evaluate the performance achievable with a given receiver model.

5. ACKNOWLEDGMENTS

This work was supported by SAMSUNG under the GRO Program, INTEL under the Doctoral Student Honor Program, the Technical University of Catalunya (UPC) and the Catalan Government (Ref. 2014SGR-1427).

6. REFERENCES

[1] S. Abadal, E. Alarcón, M. C. Lemme, M. Nemirovsky, and A. Cabellos-Aparicio. Graphene-enabled Wireless Communication for Massive Multicore Architectures. *IEEE Communications Magazine*, 51(11):137-43, 2013.

[2] S. Abadal, I. Llatser, A. Mestres, H. Lee, E. Alarcón, and A. Cabellos-aparicio. Time-Domain Analysis of Graphene-based Miniaturized Antennas for Ultra-short-range Impulse Radio Communications. *IEEE Transactions on Communications*, 63(4):1470–82, 2015.

[3] I. F. Akyildiz and J. M. Jornet. The Internet of nano-things. *IEEE Wireless Communications*, 17(6):58–63, 2010.

[4] I. F. Akyildiz, J. M. Jornet, and M. Pierobon. Nanonetworks: A New Frontier in Communications. *Communications of the ACM*, 54(11):84, 2011.

[5] F. Bonaccorso, Z. Sun, T. Hasan, and A. C. Ferrari. Graphene Photonics and Optoelectronics. *Nature Photonics*, 4:611–622, 2010.

[6] S. Deb, A. Ganguly, P. P. Pande, B. Belzer, and D. Heo. Wireless NoC as Interconnection Backbone for Multicore Chips: Promises and Challenges. *IEEE Journal on Emerging and Selected Topics in Circuits and Systems*, 2(2):228–239, 2012.

[7] C. Han, A. Ozan Bicen, and I. F. Akyildiz. Multi-Ray Channel Modeling and Wideband Characterization for Wireless Communications in the Terahertz Band. *IEEE Transactions on Wireless Communications*, 14(5):2402–2412, 2015.

[8] G. W. Hanson. Dyadic Green's Functions for an Anisotropic , Non-Local Model of Biased Graphene. *IEEE Transactions on Antennas and Propagation*, 56(3):747–757, 2008.

[9] C. Jansen, S. Priebe, and C. Moller. Diffuse scattering from rough surfaces in THz communication channels. *IEEE Terahertz Science and Technology*,1(2):462,2011.

[10] J. M. Jornet and I. F. Akyildiz. Channel Modeling and Capacity Analysis for Electromagnetic Wireless Nanonetworks in the Terahertz Band. *IEEE Transactions on Wireless Communications*, 10(10):3211–3221, 2011.

[11] J. M. Jornet and I. F. Akyildiz. Graphene-based Plasmonic Nano-Antenna for Terahertz Band Communication in Nanonetworks. *IEEE Journal on Selected Areas in Communications*, 31(12):685,2013.

[12] J. M. Jornet and I. F. Akyildiz. Femtosecond-Long Pulse-Based Modulation for Terahertz Band Communication in Nanonetworks. *IEEE Transactions on Communications*, 62(5):1742–1754, 2014.

[13] J. Kokkoniemi, J. Lehtomaki, K. Umebayashi, and M. Juntti. Frequency and Time Domain Channel Models for Nanonetworks in Terahertz Band. *IEEE Transactions on Antennas and Propagation*, 63(2):678–691, 2015.

[14] I. Llatser, C. Kremers, A. Cabellos-Aparicio, J. M. Jornet, E. Alarcón, and D. N. Chigrin. Graphene-based nano-patch antenna for terahertz radiation. *Photonics and Nanostructures - Fundamentals and Applications*, 10(4):353–358, 2012.

[15] I. Llatser, A. Mestres, S. Abadal, E. Alarcón, H. Lee, and A. Cabellos-aparicio. Time and Frequency Domain Analysis of Molecular Absorption in Short-range Terahertz Communications. *IEEE Antennas and Wireless Propagation Letters*, 14:350–353, 2015.

[16] A. F. Molisch. Ultra-Wide-Band Propagation Channels. *Proceedings of the IEEE*, 97(2):353-71, 2009.

[17] A. Shlivinski, E. Heyman, and R. Kastner. Antenna characterization in the time domain. *IEEE Transactions on Antennas and Propagation*, 45(7):1140–1149, 1997.

[18] M. Sun and Y. Zhang. Performance of intra-chip wireless interconnect using on-chip antennas and UWB radios. *IEEE Transactions on Antennas and Propagation*, 57(9):2756–2762, 2009.

[19] W. Wiesbeck, G. Adamiuk, and C. Sturm. Basic Properties and Design Principles of UWB Antennas. *Proceedings of the IEEE*, 97(2):372–385, 2009.